Thoracic Cancer

Open Access

Thoracic Cancer ISSN 1759-7706

ORIGINAL ARTICLE

Three dimensional texture analysis of noncontrast chest CT in differentiating solitary solid lung squamous cell carcinoma from adenocarcinoma and correlation to immunohistochemical markers

Rui Han[1], Roshan Arjal[2], Jin Dong[1], Hong Jiang[1], Huan Liu[3], Dongyou Zhang[1] & Lu Huang[4]

1 Department of Radiology, Wuhan No.1 Hospital, Wuhan, China
2 Department of Radiology, St. Francis Hospital, Evanston, Illinois, USA
3 GE Healthcare, Shanghai, China
4 Department of Radiology, Tongji Hospital, Tongji Medical College, Huazhong University of Science & Technology, Wuhan, China

Keywords
Adenocarcinoma; lung squamous cell carcinoma; texture analysis; tomography; x-ray computed.

Correspondence
Lu Huang, Department of Radiology, Tongji Hospital, Tongji Medical College, Huazhong University of Science & Technology, Wuhan 430030, China.
Tel: +86 27 8366 3481
Fax: +86 27 8366 2640
Email: jxmuhl@126.com; tj_lhuang@hust.edu.cn

Received: 31 May 2020;
Accepted: 8 July 2020.

doi: 10.1111/1759-7714.13592

Thoracic Cancer **11** (2020) 3099–3106

Abstract

Background: The aim of the study was to investigate 3D texture analysis (3D-TA) in noncontrast enhanced computed tomography (CT) (NCECT) to differentiate squamous cell carcinoma (SCC) from adenocarcinoma (AC), and the correlation with immunohistochemical markers.

Methods: A total of 70 patients confirmed with SCC (n = 29) and AC (n = 41) were enrolled in this retrospective study. 3D-TA was utilized to calculate TA parameters of all the tumor lesions based on NCECT images, and all the patients were divided into the training and the test groups. The TA parameters were selected by dimensionality reduction, and the model was established to differentiate SCC from AC according to the training group. The ROC curve was used to evaluate the diagnostic efficiency of the model in both the training and the test groups. Spearman correlation were used to assess the correlation between the selected feature parameters and immunohistochemical markers (P63, P40, and TTF-1).

Results: Five TA parameters, including volume count, relative deviation, Haralick correlation, gray-level nonuniformity and run length nonuniformity, were obtained to differentiate SCC from AC by multistep dimensionality reduction. The new model combined with all five TA parameters yielded a high diagnostic performance to differentiate SCC from AC (AUC 0.803) in test group, with a specificity of 89% and a sensitivity of 77%. There was weak correlation between the five texture feature parameters and P63 as well as P40 in all patients ($P < 0.05$), respectively.

Conclusions: The model including five TA parameters on NECT has a good diagnostic performance in differentiating SCC from AC.

Key points

• **Significant findings of the study**
The model created by five selected textural feature parameters can differentiate solid SCC from AC without contrast media. The selected five texture feature parameters are correlated to the immunohistochemical markers P63 and P40.
• **What this study adds**
The textural feature parameters' model can identify SCC from AC without contrast media.

Introduction

Lung cancer is one of the most common cancers, and it has the highest age-standardized rate of all cancers. It affects 22.5 lung cancer patients per 100 000 people, and remains a leading cause of death amongst cancer patients.[1, 2] Lung cancer is generally divided into small cell lung cancer and non-small cell lung cancer (NSCLC). NSCLC accounts for 80%–85% of lung cancer. The most common NSCLCs are squamous cell carcinoma (SCC) and adenocarcinoma (AC). Clinical treatment strategies are different according to the histological types of lung cancer and the choice of treatment strategies directly affects the therapeutic effect, survival rate and life quality of lung cancer patients.[3] Therefore, the early differentiation of SCC and AC is very important before treatment.

In clinical practice it is difficult to make a differential diagnosis of a solitary solid mass and nodule based on tumor morphology of traditional imaging examinations. Contrast-enhanced computed tomography (CT) scan and CT perfusion imaging can provide additional information, but the accuracy is still not high and there is limited application in patients with severe kidney dysfunction as well as contrast agent allergy. The gold standard for clinical diagnosis of lung SCC and AC is histopathology. Invasive biopsy is often used for pathological sampling. Its complications are serious, such as pneumothorax, and pulmonary hemorrhage, and the accuracy of the results is affected by sample error.[4] In recent years, textural analysis (TA) technology based on medical images has been gradually being applied in clinical practice, and has been shown to be of important value in the field of disease diagnosis, differential diagnosis and survival prediction.[5–8]

The aim of this study was to investigate whether 3D-TA based on noncontrast chest CT (NCECT) could differentiate solitary solid lung SCC and AC, and to evaluate the correlation to the immunohistochemical markers which can identify SCC from AC.

Methods

Study patients

We retrospectively collected the CT and pathological data in 88 patients with solitary solid lung cancer from 2016 to 2018 in our hospital. A flowchart of patients' enrollment is shown in Fig 1. The inclusion criteria were as follows: (i) Patients had a pathological diagnosis of SCC or AC; (ii) patients had no history of chemotherapy and/or radiotherapy; and (iii) patients had immunohistochemical markers. The exclusion criteria included the following: (i) Tumors had necrosis or calcification; (ii) tumors had atelectasis; (iii) tumors had cavitation, bubbly lucencies, and air. Finally, 70 patients (55 males, age 63 ± 9 years) were enrolled into the study, including 29 patients with lung SCC (age 66 ± 8 years), and 41 patients with AC (age 60 ± 9 years).

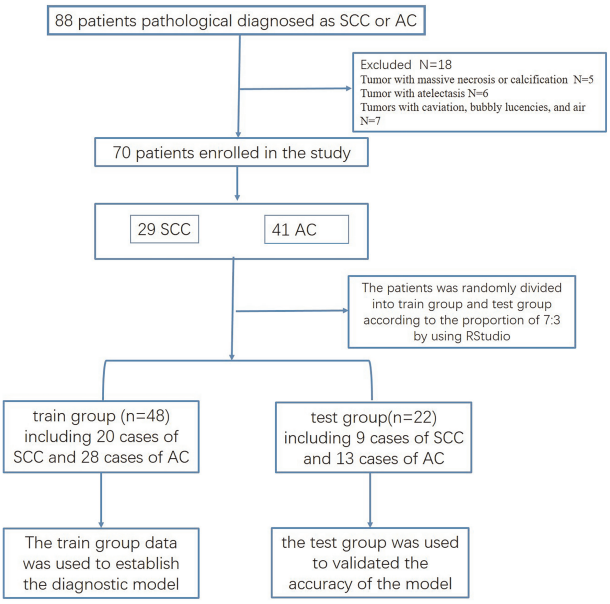

Figure 1 Flowchart of SCC and AC enrollment of patients and division of the training and test groups.

Following approval by the local institutional review board, our retrospective study was performed with a waiver of written informed consent.

CT scanning

The CT examinations of all the patients were performed on a Siemens 128-slice multidetector spiral CT (Definition AS+, Siemens, Germany). The patients were placed in a supine position on the CT table, and scanning was performed from the apex to the base of the lung with breath-holding. Scanning parameters included: voltage: 120 KV, current: 35mA; pitch: 1.2; Care Dose 4D; reconstruction thickness: 1 mm; slice interval:1 mm; Kernel: B40f medium.

3D texture analysis

The NECT images of the patients were reconstructed with 1 mm thickness and then were imported into the texture analysis software (CTKinetics APP, version V1.3.0.R, GE Healthcare). The images of lesions were drawn one slice at a time using uniform WW (220HU) and WL (35HU) in the texture analysis software. Finally, 3D merge was performed, and then the texture parameters of the tumors were calculated using the software (Fig 2). Three groups of

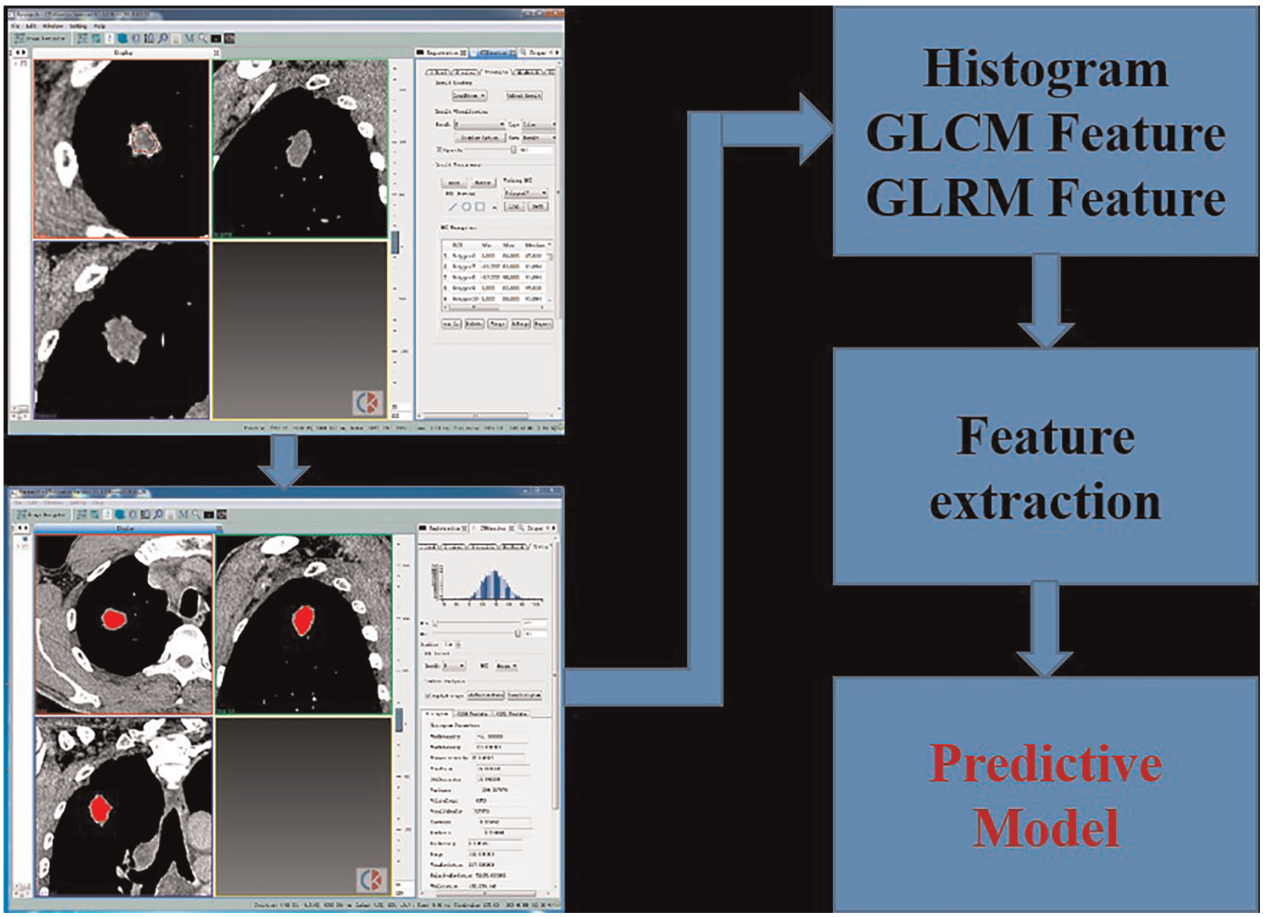

Figure 2 The workflow of 3D-TA. NECT images were imported into the texture analysis software. All lesion images were drawn one slice by one by using uniform WW (220 HU) and WL (35 HU) in the texture analysis software by experienced radiologists. 3D merge was performed, and the texture parameters of the tumors were calculated by software. A predictive model was established after extracting and filtering the texture parameters.

texture features were utilized to obtain 42 texture features parameters for each tumor. These utilized texture features were Histogram (histogram), GLCM (gray level co-occurrence matrix) and GRLM (gray level run-length matrix).

Statistical analysis

All statistical analyses were performed using RStudio 1.1.463 (Boston, Mass). The data was preprocessed, missing values were replaced by median, and then standardized to eliminate the influence of data dimension. Normal distribution was tested by Shapiro test. During texture feature's dimensionality reduction, the student's *t*-test was used to evaluate texture feature parameters satisfied the normal distribution, and wilcox test was used to evaluate texture feature parameters unsatisfied the normal distribution. Spearman correlation analysis was used to extract the texture feature parameters without high correlation. The logistic regression method was used with stepwise according to Akaike information criterion (AIC) to select the texture feature parameters for classification of SCC and AC. The diagnostic performance of selected texture parameters created model was evaluated by receiver operating characteristic (ROC) curve. Spearman correlation was performed to evaluate the relationship between texture feature parameters including in the diagnostic model and the immunohistochemical markers of lung cancer, respectively.

Results

Subject characteristics

A total of 70 patients were divided into two groups, the training group (n = 48) and the test group (n = 22), randomly (Fig 1). The training group included 20 cases of SCC and 28 cases of AC; and the test group included nine cases of SCC and 13 cases of AC. The training group data

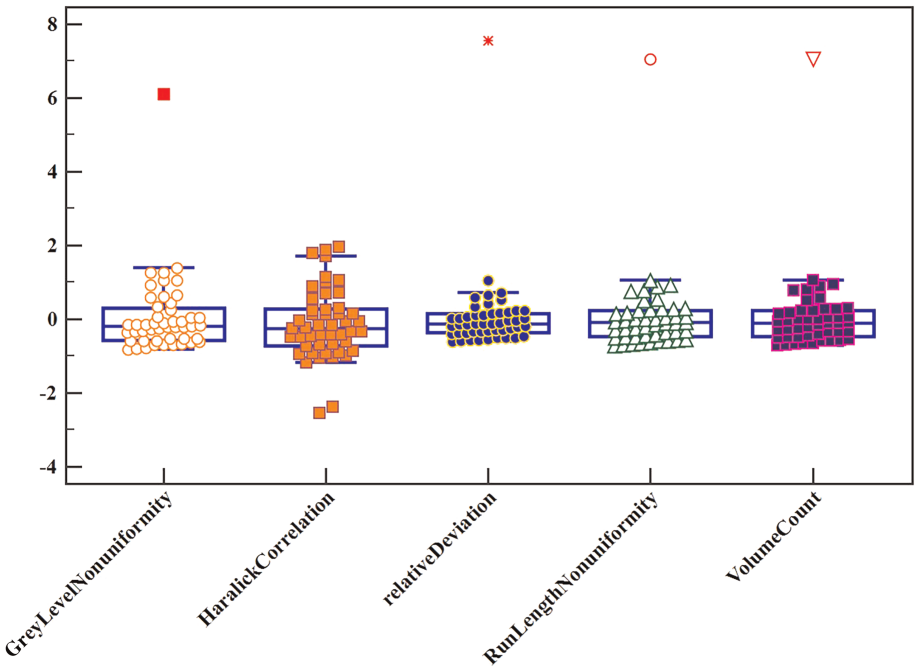

Figure 3 Five texture feature parameters, including volume count, relative deviation, Haralick correlation, gray-level nonuniformity, and run-length nonuniformity were obtained to enable a differential diagnosis of lung squamous cell carcinoma (SCC) and adenocarcinoma (AC) to be made.

was used to establish the diagnostic model, and the test group was used to validate the accuracy of the TA model.

Selection of TA parameters

Five texture feature parameters, including volume count, relative deviation, Haralick correlation, gray-level nonuniformity, and run-length nonuniformity were obtained to differentiate between SCC and AC of the lungs (Fig 3) by multistep texture feature selection and dimensional reduction described in statistical analysis session. Their sensitivity, specificity, accuracy and ROC curves are shown in Table 1 and Fig 4.

Creation and evaluation of the differential diagnostic model

Five texture feature parameters of the training set were used to establish the discriminant diagnosis model, and the model formula was as follows:

$$\begin{aligned}\text{Radscore} = {} & 0.281 + 333.147 * \mathit{VolumeCount} \\ & - 6.4088 * \mathit{relativeDeviation} \\ & + 0.992 * \mathit{HaralickCorrelation} \\ & - 6.1736 * \mathit{GrayLevelNouuniformity} \\ & - 323.813 * \mathit{RunLengthNonuniformity}\end{aligned}$$

The AUC of the model was 0.843 (95% CI: 0.725–0.961); the specificity was 85% and sensitivity 75% with a cutoff of 0.619 in the training group; and the AUC was 0.803 (95% CI: 0.576–1); the specificity was 0.889 and sensitivity 0.769 with a cutoff of 0.746 in the test group (Fig 5).

Correlation of TA parameters and immunohistochemical markers

The results of immunohistochemical markers, such as P63, P40, thyroid transcription factor-1 (TTF-1), are shown in Table 2. There was a weak correlation between the five characteristic parameters; and P63 and P40 in all patients with lung cancer, $P < 0.05$, and there was no significant correlation with TTF-1, $P > 0.05$ (Fig 6).

Discussion

The major finding of this study was that the 3D-TA model had a high diagnostic performance to differentiate solitary solid SCC from AC, and the selected five TA features correlated with the immunohistochemical markers. This model was able to identify solitary solid SCC from AC without a contrast agent, which may benefit patients with severe kidney dysfunction and contrast agent allergy.

The local irregular and macroscopic characteristics of the image is called texture. It is a rule of gray level change of pixels (or subregions) in an image which reflects the internal structure of a tissue and the heterogeneity of tumor.[9–13] The theoretical basis for this is image nonuniformity related to different genetic and pathological characteristics. Tumors have different genetic and

Table 1 The sensitivity, specificity and accuracy of the five texture feature parameters of the training and test set were respectively analyzed

	Training cohort (n = 48)			Test cohort (n = 22)		
	AUC	Sensitivity	Specificity	AUC	Sensitivity	Specificity
Volume count	0.682 (0.532, 0.809)	0.857	0.500	0.786 (0.561–0.93)	0.846	0.667
Relation deviation	0.702 (0.552, 0.825)	0.893	0.450	0.863 (0.65–0.971)	0.846	0.778
Haralick correlation	0.700 (0.551, 0.824)	0.893	0.450	0.769 (0.542–0.92)	0.769	0.778
Gray-level nonuniformity	0.677 (0.526, 0.805)	0.750	0.600	0.658 (0.428–0.844)	0.923	0.444
Run length nonuniformity	0.684 (0.532–0.809)	0.857	0.500	0.786 (0.561–0.93)	0.846	0.667

AUC, area under curve, expressed as mean (95% confidence interval).

pathological characteristics, leading to image heterogeneity. The texture feature parameters of medical images cannot be directly visualized by radiologists and they can only be identified by the texture feature extraction software. The software can accurately evaluate the image heterogeneity, and provide more information for the comprehensive evaluation of the lesions.[12, 14]

Recently, CT TA of lung tumors mainly focuses on diagnosis of benign and malignant lung masses, prediction of lymph node metastasis, diagnosis of histology and subtypes of lung cancer, evaluation of therapy effect after treatment of lung cancer and the prediction of survival rate for lung cancer.[15–20] There are few studies on histological classification of lung cancer which use different texture analysis software with different results. Basu *et al.* and others[21, 22] used 2D-TA to classify lung SCC and AC. Obviously, 2D-TA has some limitations, as it cannot fully reflect the heterogeneity of the whole tumor.

To avoid errors caused by artificial classification, random classification by 10-fold cross validation was used to classify the training and the test groups. The AUC of this 3D-TA model, including volume count, relative deviation, Haralick correlation, gray-level nonuniformity, and run length nonuniformity was 0.803, with specificity of 89% and sensitivity of 77%. Five texture parameters and model formulas were obtained for differentiating solitary solid SCC from AC. The first two texture parameters belong to histogram features, which mainly reflect the total number and relative deviation of the selected ROI pixels of images. Haralick correlation belongs to the gray level co-occurrence matrix (GLCM), which reflects the correlation of local gray level in the image. The latter two texture parameters belong to gray run length matrix (GRLM), which reflect the heterogeneity of signal and structure of image pixels in ROI. From these five parameters, we could see that there were differences in the total number of

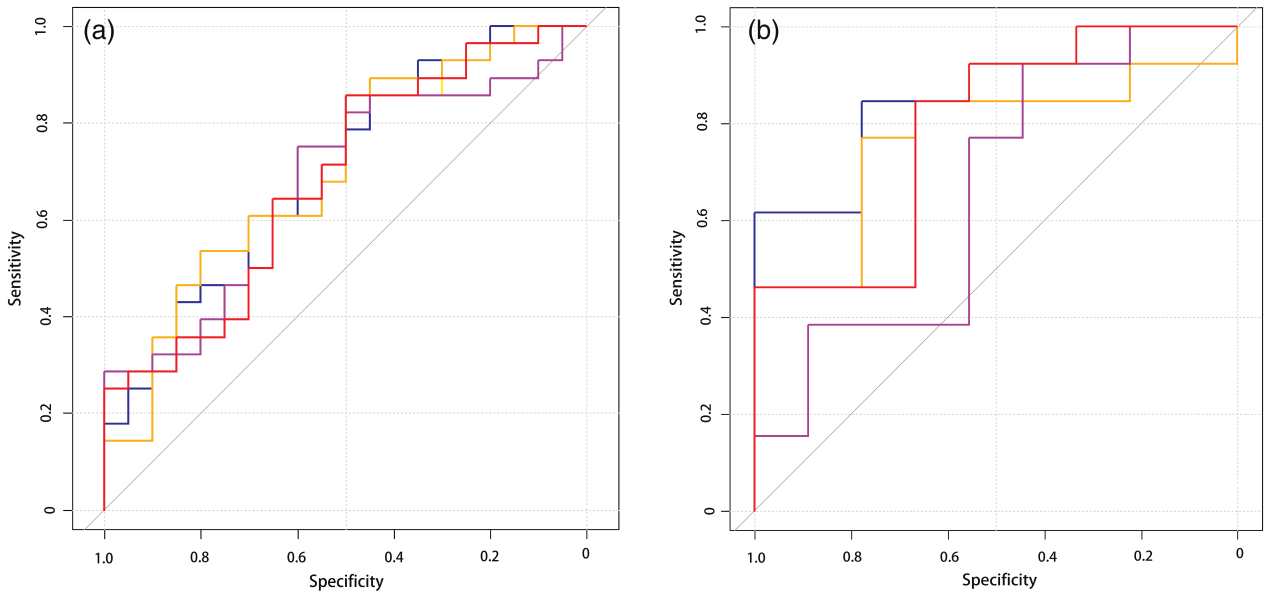

Figure 4 ROC curves of five texture feature parameters in (**a**) training set, volume count, relative deviation, Haralick correlation, gray-level nonuniformity, run-length nonuniformity, and (**b**) test set, volume count, relative deviation, Haralick correlation, gray-level nonuniformity, run-length nonuniformity, respectively.

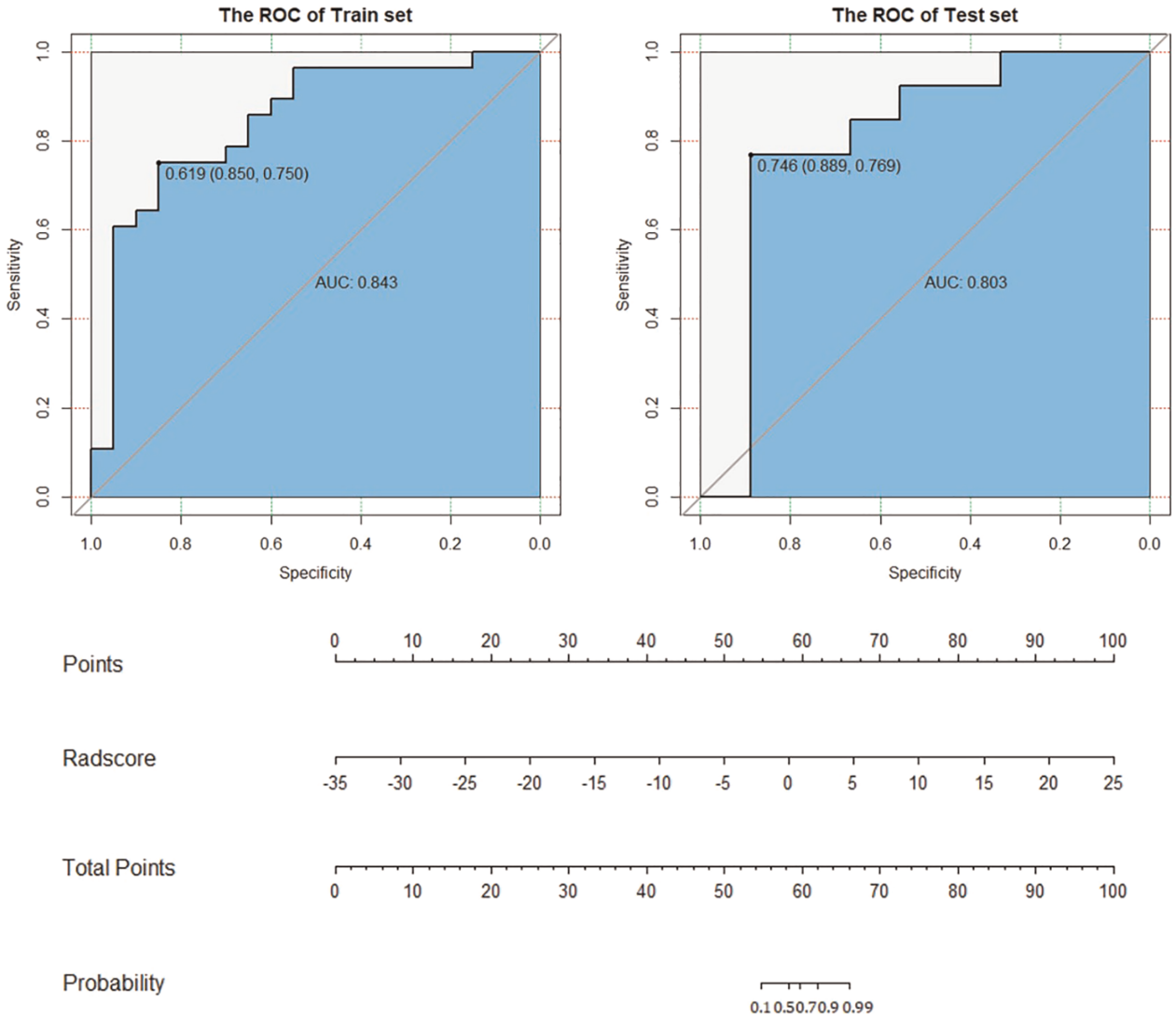

Figure 5 The training set and testing set ROC curves of the model. In this model, the AUC was 0.803 in the test set; specificity was 89% and sensitivity 77%. The cutoff was 0.746.

pixels, the correlation of signal and gray level, and the structure of SCC and AC in NECT images. The theoretical basis for these findings may reflect the heterogeneity of tumor pathological manifestation.

Table 2 Expression of immunohistochemical markers (P63, P40, TTF-1) in all patients

Immunohistochemical markers	SCC (*n* = 29)	AC (*n* = 41)
P63 (+), *n* (%)	28 (97%)	9 (22%)
P40 (+), *n* (%)	28 (97%)	0 (0%)
TTF-1 (+), *n* (%)	2 (5%)	31 (76%)

Immunohistochemical markers expressed as count (percentage). TTF-1, Thyroid transcription factor-1.

Immunohistochemical markers of lung cancer, such as P63, P40 and TTF-1, are considered as the gold standard in the differentiation of SCC from AC. The correlation between the three immunohistochemical markers and the selected five texture parameters enabled us to verify our TA model. P63 and P40 are immunohistochemical markers of SCC, and TTF-1 is a marker of AC, and they have a high degree of accuracy, specificity and sensitivity in differentiating SCC from AC.[23–25] The selected five texture parameters were weakly correlated with P63 and P40, but not with TTF-1. It is speculated that these five texture parameters may reflect the histopathological characteristics of SCC, which is the histological basis for the differentiation SCC from AC. As each texture parameter may

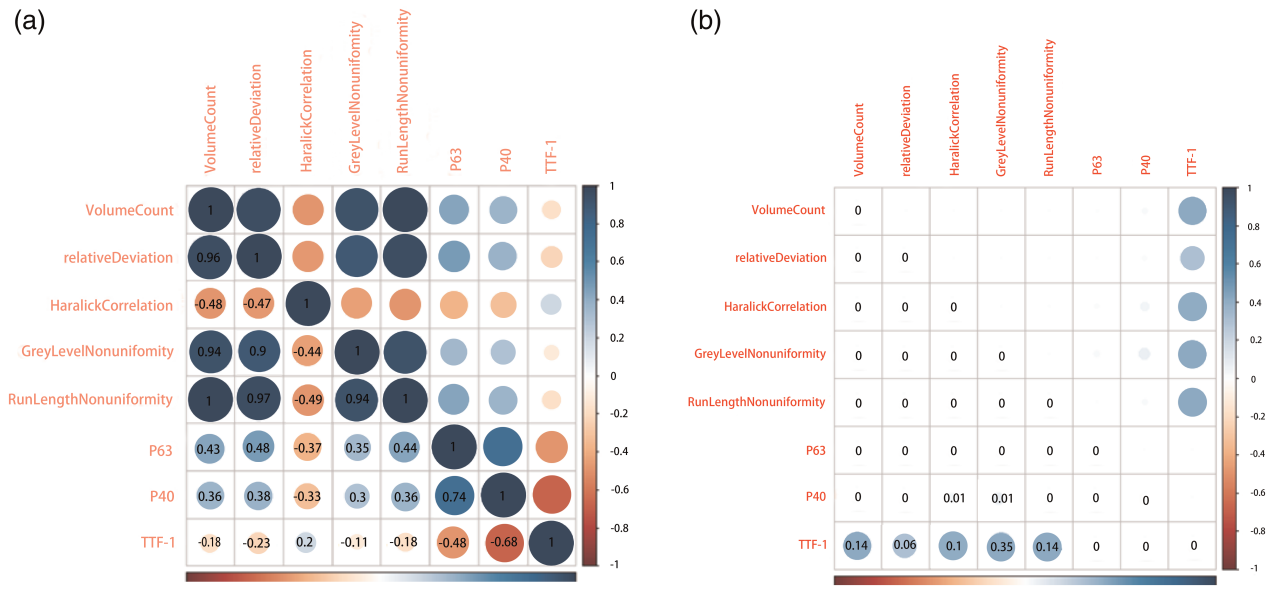

Figure 6 Heatmaps of correlation coefficient and *P*-value. Spearman correlation analysis showed there was a weak correlation between the five characteristic parameters and P63 and P40 in all patients with lung cancer, $P < 0.05$, but not with TTF-1, $P > 0.05$.

represent tumor cell type, density and vascular density and so on, further studies with a larger sample size and correlation with histopathology is needed.

There are some limitations in this study. First, the sample size was relatively small, and it was a retrospective analysis. A larger sample size will be enrolled in the next study and our model for the differential diagnosis of SCC and AC of the lungs will also be validated and improved. Second, only the immunohistochemical markers P63, P40 and TTF-1 were included in this study. Other texture parameters that correlate with the other immunohistochemical markers need further research. Third, NECT images of lung cancer patients were performed on one CT scanner, and external validation will be investigated on CT images of the other CT scanners.

In conclusion, this 3D-TA model, including volume count, relative deviation, Haralick correlation, gray-level nonuniformity, and run length nonuniformity on NECT images had high specificity, sensitivity and accuracy to differentiate solitary solid SCC from AC. The five texture feature parameters correlated with immunohistochemical markers P63 and P40. This TA model may provide important clinical value in the diagnosis and treatment of SCC and AC patients in the future.

Acknowledgments

This work was supported by Key Program of Wuhan Municipal Health Commission project (grant numbers: WX18B08, 2018).

Disclosure

No authors report any conflict of interest.

References

1 Ding N, Zhou N, Zhou M, Ren GM. Respiratory cancers and pollution. *Eur Rev Med Pharmacol Sci* 2015; **19**: 31–7.
2 Fitzmaurice C, Dicker D, Pain A *et al.* The global burden of cancer 2013. *JAMA Oncol* 2015; **1**: 505–27.
3 Chan BA, Hughes BG. Targeted therapy for non-small cell lung cancer: Current standards and the promise of the future. *Transl Lung Cancer Res* 2015; **4**: 36–54.
4 Khan T, Usman Y, Abdo T, Chaudry F, Keddissi JI, Youness HA. Diagnosis and management of peripheral lung nodule. *Ann Transl Med* 2019; **7**: 348–8.
5 Yang F, Young LA, Johnson PB. Quantitative radiomics: Validating image textural features for oncological PET in lung cancer. *Radiother Oncol* 2018; **129**: 209–17.
6 Yang Y, Yan LF, Zhang X *et al.* Optimizing texture retrieving model for multimodal MR image-based support vector machine for classifying glioma. *J Magn Reson Imaging* 2019; **49**: 1263–74.
7 Zhang S, Chiang GC, Magge RS *et al.* Texture analysis on conventional MRI images accurately predicts early malignant transformation of low-grade gliomas. *Eur Radiol* 2019; **29**: 2751–9.
8 Ho LM, Samei E, Mazurowski MA *et al.* Can texture analysis be used to distinguish benign from malignant adrenal nodules on unenhanced CT, contrast-enhanced CT, or in-phase and opposed-phase MRI? *Am J Roentgenol* 2019; **212**: 554–61.

9 Qin C, Yao D, Shi Y, Song Z. Computer-aided detection in chest radiography based on artificial intelligence: A survey. *Biomed Eng Online* 2018; **17**: 113.
10 Varghese BA, Cen SY, Hwang DH, Duddalwart VA. Texture analysis of imaging: What radiologists need to know. *Am J Roentgenol* 2019; **212**: 520–8.
11 Dennie C, Thornhill R, Souza CA *et al*. Quantitative texture analysis on pre-treatment computed tomography predicts local recurrence in stage I non-small cell lung cancer following stereotactic radiation therapy. *Quant Imaging Med Surg* 2017; **7**: 614–22.
12 Gillies RJ, Kinahan PE, Hricak H. Radiomics: Images are more than pictures, they are data. *Radiology* 2016; **278**: 563–77.
13 Lubner MG, Smith AD, Sandrasegaran K, Sahani DV, Pickhardt PJ. CT texture analysis: Definitions, applications, biologic correlates, and challenges. *Radiographics* 2017; **37**: 1483–503.
14 Wu K, Garnier C, Coatrieux JL, Shu H. A preliminary study of moment-based texture analysis for medical images. *Conf Proc IEEE Eng Med Biol Soc* 2010; **2010**: 5581–4.
15 Hassani C, Varghese BA, Nieva J, Duddalwar V. Radiomics in pulmonary lesion imaging. *Am J Roentgenol* 2019; **212**: 497–504.
16 Beig N, Khorrami M, Alilou M *et al*. Perinodular and intranodular radiomic features on lung CT images distinguish adenocarcinomas from granulomas. *Radiology* 2019; **290**: 783–92.
17 Durot C, Mule S, Soyer P, Marchal A, Grange F, Hoeffel C. Metastatic melanoma: Pretreatment contrast-enhanced CT texture parameters as predictive biomarkers of survival in patients treated with pembrolizumab. *Eur Radiol* 2019; **29**: 3183–91.
18 LN E, Zhang N, Wang RH, Wu Z. Comparative analysis of computed tomography texture features between pulmonary inflammatory nodules and lung cancer. *Zhonghua Zhong Liu Za Zhi* 2018; **40**: 847–50.
19 Ravanelli M, Agazzi GM, Ganeshan B *et al*. CT texture analysis as predictive factor in metastatic lung adenocarcinoma treated with tyrosine kinase inhibitors (TKIs). *Eur J Radiol* 2018; **109**: 130–5.
20 Starkov P, Aguilera TA, Golden DI *et al*. The use of texture-based radiomics CT analysis to predict outcomes in early-stage non-small cell lung cancer treated with stereotactic ablative radiotherapy. *Br J Radiol* 2019; **92**: 20180228.
21 Basu S, Hall LO, Goldgof D *et al*. Developing a classifier model for lung tumors in CT-scan images. *2011 IEEE International Conference on Systems, Man, and Cybernetics*. Anchorage, AK, 2011; 1306–1312.
22 Liu H, Jing B, Han W, Long Z, Mo X, Li H. A comparative texture analysis based on NECT and CECT images to differentiate lung adenocarcinoma from squamous cell carcinoma. *J Med Syst* 2019; **43**: 59.
23 Affandi KA, Tizen NMS, Mustangin M, Zin RRMR. P40 immunohistochemistry is an excellent marker in primary lung squamous cell carcinoma. *J Pathol Transl Med* 2018; **52**: 283–9.
24 Gailey MP, Bellizzi AM, Jensen CS. Differentiating small cell carcinoma from squamous cell carcinoma in cytologic specimens: A head-to-head comparison of p40 and p63 using cell block immunocytochemistry. *Appl Immunohistochem Mol Morphol* 2016; **24**: 11–5.
25 Gurgus D, Grigoras ML, Motoc AGM *et al*. Clinical relevance and accuracy of p63 and TTF-1 for better approach of small cell lung carcinoma versus poorly differentiated nonkeratinizing squamous cell carcinoma. *Rom J Morphol Embryol* 2019; **60**: 139–43.

